UNIVERSITÀ DI PARMA

ARCHIVIO DELLA RICERCA

University of Parma Research Repository

An engineered anti-idiotypic antibody-derived killer peptide (KP) early activates swine inflammatory monocytes, CD3+CD16+ natural killer T cells and CD4+CD8α+ double positive CD8β+ cytotoxic T lymphocytes associated with TNF-α and IFN-γ secretion

This is the peer reviewd version of the followng article:

Original
An engineered anti-idiotypic antibody-derived killer peptide (KP) early activates swine inflammatory monocytes, CD3+CD16+ natural killer T cells and CD4+CD8α+ double positive CD8β+ cytotoxic T lymphocytes associated with TNF-α and IFN-γ secretion / Ferrari, L.; Martelli, P.; Saleri, R.; De Angelis, E.; Ferrarini, G.; Cavalli, V.; Passeri, B.; Bazzoli, G.; Ogno, G.; Magliani, W.; Borghetti, P.. - In: COMPARATIVE IMMUNOLOGY, MICROBIOLOGY AND INFECTIOUS DISEASES. - ISSN 0147-9571. - 72:(2020), pp. 1-15. [10.1016/j.cimid.2020.101523]

Availability:
This version is available at: 11381/2900169 since: 2021-10-15T11:42:48Z

Publisher:

Published
DOI:10.1016/j.cimid.2020.101523

Terms of use:

Anyone can freely access the full text of works made available as "Open Access". Works made available

Publisher copyright

note finali coverpage

(Article begins on next page)

02 August 2024

An engineered anti-idiotypic antibody-derived killer peptide (KP) early activates swine inflammatory monocytes, CD3$^+$CD16$^+$ natural killer T cells and CD4$^+$CD8α$^+$ double positive CD8β$^+$ cytotoxic T lymphocytes associated with TNF-α and IFN-γ secretion

Luca Ferrari [a,*], Paolo Martelli [a], Roberta Saleri [a], Elena De Angelis [a], Giulia Ferrarini [a], Valeria Cavalli [a], Benedetta Passeri [a], Gianluca Bazzoli [a], Giulia Ogno [a], Walter Magliani [b], Paolo Borghetti [a]

[a] Department of Veterinary Science, University of Parma, Strada del Taglio, 10 – 43126, Parma, Italy
[b] Department of Medicine and Surgery, University of Parma, Via Gramsci, 14 – 43126, Parma, Italy

A R T I C L E   I N F O

A B S T R A C T

This study evaluated the early modulation of the phenotype and cytokine secretion in swine immune cells treated with an engineered killer peptide (KP) based on an anti-idiotypic antibody functionally mimicking a yeast killer toxin. The influence of KP on specific immunity was investigated using porcine reproductive and respiratory syndrome virus (PRRSV) and porcine circovirus type 2 (PCV2) as ex vivo antigens. Peripheral blood mononuclear cells (PBMC) from healthy pigs were stimulated with KP and with a scramble peptide for 20 min, 1, 4 and 20 h or kept unstimulated. The cells were analyzed using flow cytometry and ELISA. The same time-periods were used for KP pre-incubation/co-incubation to determine the effect on virus-recalled interferon-gamma (IFN-γ) secreting cell (SC) frequencies and single cell IFN-γ productivity using ELISPOT. KP induced an early dose-dependent shift to pro-inflammatory CD172α$^+$CD14^{+high} monocytes and an increase of CD3$^+$CD16$^+$ natural killer (NK) T cells. KP triggered CD8α and CD8β expression on classical CD4$^-$CD8αβ$^+$ cytotoxic T lymphocytes (CTL) and double positive (DP) CD4$^+$CD8α$^+$ Th memory cells (CD4$^+$CD8α^{+low} CD8β^{+low}). A fraction of DP cells also expressed high levels of CD8α. The two identified DP CD4$^+$CD8α^{+high} CD8β$^{+low/+high}$ CTL subsets were associated with tumor necrosis factor alpha (TNF-α) and IFN-γ secretion. KP markedly boosted the reactivity and cross-reactivity of PRRSV type-1- and PCV2b-specific IFN-γ SC. The results indicate the efficacy of KP in stimulating Th1-biased immunomodulation and support studies of KP as an immunomodulator or vaccine adjuvant.

1. Introduction

Several antibody (Ab)-derived small peptides display an intrinsically wide spectrum of activity in vitro and in vivo against distinct infectious pathogens. In humans, these molecules may act as a type of natural defense system, together with endogenous antimicrobial peptides (AMP) that include α- and β-defensins, cathelicidins, and granulysin [1], natural Abs, and other soluble inflammatory/immune factors such as lipopolysaccharide binding protein (LBP) and the complement system [2]. Among these peptides, Ab fragments and anti-idiotypic Ab-derived killer toxin functional mimotopes have been studied for their potential use as anti-infective compounds against microbial and viral agents responsible for major infections in humans and domestic animals. AKVTMTCSAS is the first engineered anti-idiotypic Ab-derived killer peptide (KP) shown to have significant antimicrobial effect in vitro against *Candida* spp*., Cryptococcus neoformans, Paracoccidioides brasiliensis, Acanthamoeba castellanii, Leishmania major and Leishmania infantum, Toxoplasma gondii*, and *Malassezia pachydermatis* [3–10]. KP proved to display inhibitory activity against human immunodeficiency virus type 1 (HIV-1), human and avian influenza A viruses, and herpes simplex virus type 1 (HSV-1) in vitro and in vivo [11–13].

However, information on the immunomodulatory properties of KP are scarce. It was demonstrated that KP displays immunomodulatory activity by interacting with murine innate immune cells such as dendritic cells (DC) and macrophages via receptors involved in immune cell inter-communication (SIGN-R1, MHC-II, CD16, CD32). These interactions result in the up-regulation of the co-receptors CD8α, CD80, and CD40, which in turn, can trigger lymphocyte activation and cytokine release [14]. Different mechanisms of action are involved in this wide spectrum of activity, in part owing to the ability of KP to spontaneously and reversibly self-assemble and slowly release its dimeric form over time and to interact, for example in fungi such as *Candida albicans*, with specific β-1,3-glucan containing cell wall receptors [15–18].

The pig is a potentially interesting species with regard to addressing KP modulation of the immune system, since pigs share several important immunological features with humans [19,20].

For example, porcine blood CD172α⁺CD14⁺ monocytes, which can up-regulate CD14 expression upon stimulation (CD14^{+high}) monocytes in terms of genes related to immune activation [21]. These cells are involved in the first line of defense against different pathogens by evolving to macrophages, acting as antigen presenting cells (APC), displaying natural recognition mechanisms, chemotaxis to inflammatory sites and inducing inflammatory reactions due to the interaction between CD14 and the lipopolysaccharide (LPS) of gram-negative bacteria. They can express chemokines/chemokine receptors including C-C chemokine receptore type 1 (CCR1), interleukin (IL)-8RB/R2, and C-X-C motif chemochine receptor 2 (CXCR2); release pro-inflammatory cytokines including tumor necrosis factor-alpha (TNF-α) and IL-18; and express inflammatory molecules (e.g. S100A8)/recruit neutrophils [21].

Natural killer (NK) cells act using innate recognition/cytotoxic mechanisms which share with NKT cells. These mechanisms include recognition of Ab-opsonized cells by CD16, an activating receptor (FcγRIII) involved in Ab-dependent cell-mediated cytotoxicity (ADCC), and the release of perforins and granzymes that mediate direct cell killing and apoptosis of virus-infected cells and cancer cells. The activity of these cells is triggered by innate cells such as macrophages or T lymphocytes that produce TNF-α and interferon-gamma (IFN-γ), respectively [22]. NKT cells are also involved in anti-viral response regulation [23,24]. Considering that porcine and human NKT cells share several features [25,26], the porcine model could be promising for comparative studies.

Proper activation and amplification of the immune response are dependent on T helper (Th) lymphocytes, which can be influenced by the extent and features of innate cell reactivity and APC, leading to the secretion of a variety of cytokines [20,27]. Th1 lymphocytes are involved in the anti-viral responses where IFN-γ plays a key role in sus-

taining both innate functionality and the efficiency of adaptive immune T cells, such as "classical" CD4⁻CD8α^{+high}CD8β⁺ cytotoxic T lymphocytes (CTL) and double positive (DP) CD4⁺CD8α⁺ memory T cells, which are present in relatively high numbers in pig blood [28,29]. The activation status of these subsets and their interplay is crucial during both the early phase of many viral infections and also the late phase for complete clearance or virus control [23,30–33]. Up-regulation of CD8α can occur in T lymphocytes in response to different antigenic stimuli and can be used to evaluate an activated status [22,27,34]. Interestingly, porcine CD4⁺CD8α⁺ DP CTL expressing CD8β have been so far detected in immune pigs [22]. Upon viral infections caused by Aujeszky's disease virus (ADV) [35], classical swine fever virus (CSFV) [31], African swine fever virus (ASFV) [32], and porcine reproductive and respiratory syndrome virus type 2 (PRRSV-2) [36], DP CTL have been related to a polyfunctional phenotype, displaying both memory and cytotoxic functions through the secretion of granzyme B, perforin and IFN-γ.

In a previous study in adult pigs [37], we found that prolonged treatment with KP induced a wide range of immune modulation in both innate and adaptive immune cells within peripheral blood mononuclear cells (PBMC). A dose-dependent shift in quiescent circulating monocytes to a pro-inflammatory CD172α⁺CD14^{+high} phenotype was observed together with an increase of CD3⁺CD16⁺ NKT cells. Furthermore, the reduction of naïve CD4⁺CD8α⁻ Th lymphocytes was associated with the up-regulation of CD8α on CD4⁺CD8α⁺ memory Th cells. Activated CD25⁺CD16⁺ cells and classical CD8β⁺ CTL also increased following prolonged KP exposure [37].

The present study investigates the early in vitro immunomodulatory effects of KP on innate immune cells and acquired T lymphocyte subpopulations in terms of phenotypical/functional changes and cytokine secretion. These assessments can reveal important properties and effects of the engineered Ab-derived peptide on pivotal immune subsets.

Furthermore, an ELISPOT assay was used to evaluate the potential immunomodulatory effects of KP on virus-specific homologous and heterologous IFN-γ secreting cell (SC) ex vivo recalled responses in pigs vaccinated against PRRSV and porcine circovirus type 2 (PCV2), which are predominant pig pathogens.

2. Materials and methods

2.1. Animals and sample collection

PBMC were collected from healthy adult hybrid pigs from two conventional commercial herds in Northern Italy. Animals were intramuscularly vaccinated at weaning against PRRSV (MLV PRRSV-1 DV strain-based Porcilis® PRRS vaccine; MSD-Animal Health, Whitehouse Station, NJ, USA) and PCV2 (subunit PCV2a Cap-based Porcilis® PCV vaccine; MSD-Animal Health), as previously described [33,38]. The absence of PRRSV and PCV2 infections was confirmed in blood samples by reverse transcription-quantitative PCR (RT-qPCR) and qPCR, respectively, according to previously established protocols [30]. The absence of PRRSV infection was also assessed by serology. *Mycoplasma hyopneumoniae* negativity was checked by serology. A group of 10 animals was kept unvaccinated for both antigens and served as the negative control group for quantification of virus-specific IFN-γ SC. All pigs of the unvaccinated group were tested for the same pathogens and confirmed as negative. Blood samples were collected in lithium heparin and kept at room temperature with gentle agitation until processed for PBMC isolation within 4 h. Two independent experiments were carried out on 10 animals for each experiment.

2.2. Killer peptide (KP)

The KP, also defined as A-10-S (AKVTMTCSAS), MW 998.18 Da, pI 8.27, was synthesized as a dimer by Fmoc solid-phase peptide synthesis (SPPS). The lyophilized powder was dissolved in dimethylsulfoxide (DMSO) at 20 mg/mL (Sigma-Aldrich, St. Louis, MO, USA) and prop-

erly diluted before use. Controls included unstimulated cells (negative control containing the same dilution of DMSO) and cells incubated with a synthesized scramble peptide based on the KP sequence (SP, MSTAVSKCAT) in DMSO in order to exclude a response to an irrelevant peptide [39]. Peptide purity was checked by high performance liquid chromatography (HPLC). The purity was > 95 % for both KP and SP.

2.3. Isolation of porcine PBMC

PBMC were isolated by Histopaque-1077® density gradient (Sigma-Aldrich) as previously described [38]. The cells were washed twice with sterile PBS + 1% heat inactivated (hi) foetal bovine serum (FBS) and suspended in complete RPMI-1640 (cRPMI-1640) + 10 % DMSO + 40 % hi FBS (Gibco, Carlsbad, CA, USA). Each suspension was frozen at −80 °C and stored in liquid nitrogen. Thawed cells were washed twice with cRPMI-1640 + 10 % hi FBS, resuspended in the same medium, and checked for viability based on Trypan blue exclusion (Sigma-Aldrich). Cell viability was > 90 % in all samples prior to stimulation with KP or SP and subsequent analyses.

2.4. Lymphoproliferation/cytotoxicity assay with KP

An assay based on 3-(4,5-dimethylthiazol-2-yl)-2,5-diphenyltetrazolium bromide (MTT; Sigma-Aldrich) was performed to evaluate lymphoproliferation/metabolic activity and cytotoxicity upon KP treatment. Briefly, PBMC were plated at 2×10^5 cells/well (100 μL) in flat-bottom 96-well plates in duplicate and incubated for 48 and 72 h. Incubation with phytohemagglutinin (PHA, 5 μg/mL) was used as the positive control. During the last 3 h, 10 μl of 5 mg/mL MTT in sterile PBS were added. After incubation, 100 μl of 0.01 N HCl + 10 % sodium dodecyl sulfate (SDS) were added to develop the reaction. After overnight incubation, plates were read using a Victor-3™ 1420 Multilabel Counter (PerkinElmer, Waltham, MA, USA) and stimulation indexes were calculated as the ratios between the optical density at 540 nm (OD_{540nm}) in PHA-, SP-, or KP-stimulated cells and OD_{540nm} in unstimulated cells (negative control) after subtraction of the mean value in the cell-free control and the OD_{690nm} value (reference value).

2.5. Analysis of immune subsets in PBMC upon KP stimulation

The effect of KP stimulation was evaluated in vitro on immune subsets within PBMC by flow cytometry (FCM) using previously established protocols [23,29,30,33,37,40]. Briefly, PBMC (1×10^6 cells/ mL) were incubated in snap-cap tubes (Sarstedt, Nümbrecht, Germany) in cRPMI-1640 + 10 % hi FBS for 20 h with the addition of 0, 10, 20, and 40 μg/mL KP or SP for the whole period or for the last 4 h, 1 h, and 20 min, at 37 °C, 5% CO_2.

After stimulation, samples were surface stained for CD172α/CD14, CD3/CD4, CD3/CD8α, CD3/CD8β, CD4/CD8α/CD8β, and CD3/CD16. The details of the reagents used for FCM analysis are provided in Table 1. The phenotypes of the immune subsets analyzed are listed in Table 2. Negative controls consisted in unstained PBMC or PBMC incubated with secondary Ab. Fluorescence-minus-one (FMO) controls were included for each staining combination. CD8β staining was performed by incubating cells with the specific primary Ab followed by the secondary Ab for 15 min on ice, before adding Abs for the other markers.

The analysis of CD16+ cells was related to NK (CD3⁻) and NKT (CD3⁺) subsets by evaluating cells in the lymphocyte gate [22,24]. Cell samples were also stained with 1/1000 Sytox® AADvanced™ (Invitrogen, Paisley, UK) to exclude dead cells from the analysis, which comprised < 20 % in all samples, independent from KP concentration. The analysis was performed using a Cytomics FC500 dual laser flow cytometer and CXP software (Beckman Coulter, Indianapolis, IN, USA) based on doublet discrimination, live cells, and lymphocyte or PBMC (extended to include monocytes) gating after acquisition of at least 40 000 cell events (Fig. 1).

Washes after each surface staining were performed with 2 mL of PBS + 1 % hi FBS except for the step before/after Sytox AADvanced, in which PBS was used according to the manufacturer's recommendations.

Cell analysis was performed to evaluate and quantify the cellular responses to KP. The responses are expressed as percentages. The levels of all cell subsets incubated with KP were compared to the levels of unstimulated cells and SP-incubated cells. As the unstimulated cell values and SP-incubated cell values were almost identical (and therefore not statistically different), only the values in unstimulated samples are shown in each figure.

2.6. Quantification of cytokine release in supernatants of KP-stimulated PBMC

PBMC were incubated in 24-well plates (4×10^6 cells/mL) for 20 h with the addition of 0, 10, 20, and 40 μg/mL KP or SP for the whole period or for the last 4 h, 1 h, and 20 min, at 37 °C, 5% CO_2. The samples were then centrifuged at 400 ×g and supernatants were collected to evaluate IFN-α, TNF-α, IFN-γ, and IL-10 secretion. Cytokine concentrations were quantified using commercial species-specific solid-phase sandwich ELISA kits (swine TNFα, IFN-γ, and IL-10 ELISA Kits, Thermo Fisher Scientific – Life Technologies, Carlsbad, CA, USA; RayBio® Porcine IFN-alpha ELISA Kit, RayBiotech, Norcross, GA, USA) and a Victor-3™ 1420 Multilabel Counter equipped with a 450 nm filter (PerkinElmer, Waltham, MA, USA). Lower limits of detection (LLD) were < 3 pg/mL, 2 pg/mL, < 3 pg/mL, and 36 pg/mL for each kit, respectively.

Table 1

Staining reagents used in flow cytometry. Antigen, clone/cell line and isotype refer to the reactivity and characterization of the primary fluorochrome-labelled or unlabelled antibody. Sytox AADvanced was used to discriminate between viable and dead cells.

Staining	Clone/cell line	Isotype	Source	Fluorochrome	Secondary antibody
CD172α	74-22-15	IgG1κ	Southern Biotech	PE	
CD14	MIL2	IgG2b	Serotec	FITC	
CD16 (FcRIII)	G7	IgG1	Serotec	FITC	
CD3ε	PPT3	IgG1κ	Southern Biotech	FITC or PE	
CD4	74-12-4	IgG2bκ	Southern Biotech	PE	
CD8α	76-2-11	IgG2aκ	Southern Biotech	FITC	
CD8β	PG164A	IgG2a	Kingfisher Biotech	unlabelled	goat anti-mouse IgG2aγ-PE/Cy7 (1080-17, Southern Biotech)
Sytox AADvanced (viable/dead cells)			Invitrogen	FL4 channel fluorescence	

PE: phycoerythrin; FITC: fluorescein isothiocyanate; FcRIII: fragment constant receptor 3; F(ab')₂: divalent fragment antigen-binding; PE/Cy7: phycoerythrin/cyanin 7; Southern Biotech, Birmingham, AL, USA; Kingfisher Biotech Inc., St. Paul, MN, USA; Dako Cytomation, Glostrup, Denmark; AbD Serotec, Raleigh, NC, USA; Invitrogen, Paisley, UK.

Table 2

Phenotypes of the immune cell subsets analyzed by flow cytometry. The details for each staining reagent and analysis are provided in the materials and methods section and Table 1.

Immune cell subset	Phenotype
Monocytes	CD172α $^+$CD14 $^{+low/high}$
NK cells	CD3 $^-$CD16 $^+$
NKT cells	CD3 $^+$CD16 $^+$
Total CD4 + T lymphocytes	CD3 $^+$CD4 $^+$
Total CD8α + T lymphocytes	CD3 $^+$CD8α $^+$
Naïve T helper lymphocytes	CD4 $^+$CD8α $^-$CD8β $^-$
Memory T helper cells	CD4 $^+$CD8α $^+$CD8β $^-$
Cytotoxic T lymphocytes	CD3 $^+$CD8β $^+$CD4 $^-$CD8α $^{+high}$ CD8β $^+$
Double positive (DP) cytotoxic T lymphocytes	CD4 $^+$CD8α $^{+low/high}$ CD8β $^{+low/high}$
Viable/dead cells	Sytox AADvanced (included in all staining combinations)

2.7. Quantification of PRRSV-specific and PCV2-specific IFN-γ SC frequencies and single cell IFN-γ productivity in KP-stimulated PBMC

The effect of KP was tested on the ex vivo recall response of virus-specific IFN-γ SC to PRRSV-1 strains and PCV2b strains by ELISPOT, based on previously established protocols [30,33,38,41]. Specifically, PBMC were pre-stimulated for 20 min, 1, 4, and 20 h with KP or SP during a 20-h pre-incubation step in snap-cap tubes. The cells were then plated in duplicate (4×10^5 cells/well) in cRPMI-1640 + 10 % FBS in MultiScreen® HTS-IP 96-well plates (Merck Millipore, Darmstadt, Germany), or were stimulated directly in the ELISPOT plate for 20 h at 37 ˚C, 5% CO_2, with KP or SP alone, KP or SP and each PRRSV-1 vaccine (Porcilis® PRRS, MSD-AH; Unistrain® PRRS, Laboratorios Hipra S.A., Girona, Spain), or the BS/114/S and BS/55 PRRSV-1 isolates [38] (provided by Dr. Ferrari M. and Dr. Dotti S., IZSLER Brescia, Italy), the PCV2b I12/11-10K15 and PCV2b Bakker-11D26 isolates (provided by Dr. Fachinger V. and Dr. Witvliet M.H., MSD-AH, Boxmeer, Belgium), or with each virus alone (Table 3). As posi-

tive controls, 4×10^5 PBMC/well were incubated with PHA (5 μg/mL). As negative controls, 4×10^5 PBMC were incubated without any antigen or KP, and their values were subtracted from all stimulation conditions.

The results are shown in terms of differential increase (delta, Δ) calculated for each pig as IFN-γ SC frequency in KP + PRRSV or KP + PCV2 stimulated sample after subtraction of the value in the corresponding PRRSV-alone or PCV2-alone stimulated sample and in the KP-alone stimulated sample. To better highlight the extent of the effect of KP on the ELISPOT responses, the percentage increase in PRRSV + KP and PCV2 + KP stimulated cells was calculated by dividing the differential increase (or delta value) by the value in PRRSV + KP or PCV2 + KP stimulated cells and multiplying by 100. In addition, visual analysis of IFN-γ spots was performed to evaluate single cell IFN-γ productivity related to spot size and intensity, depending on the amount of cytokine secreted by each single re-activated T cell.

2.8. Statistical analysis

Statistical analysis was performed using Analysis of Variance (ANOVA) and Paired Student's *t*-test for ELISPOT as previously described [42]. The Mann-Whitney and Kruskal-Wallis tests were used for the other analyses to compare the different in vitro stimulation conditions. A p-value < 0.05 was considered significant. Statistical analysis was carried out using the SPSS System for Windows v.14.0 (IBM, Armonk, NY, USA).

3. Results

3.1. Lymphoproliferation/cytotoxicity evaluation

Stimulation of porcine PBMC with KP or SP did not elicit any lymphoproliferation or significant cytotoxicity at 48 or 72 h. As the cell responsiveness control, stimulation with PHA at both times confirmed significant increases of the stimulation indexes (SI) in all samples (SI_{48h} = 2.21–4.48; SI_{72h} = 7.81–32.36). Rosette formation representing morphofunctional aggregation of activated cells was evident. Unstimulated PBMC did not show any significant response (data not shown).
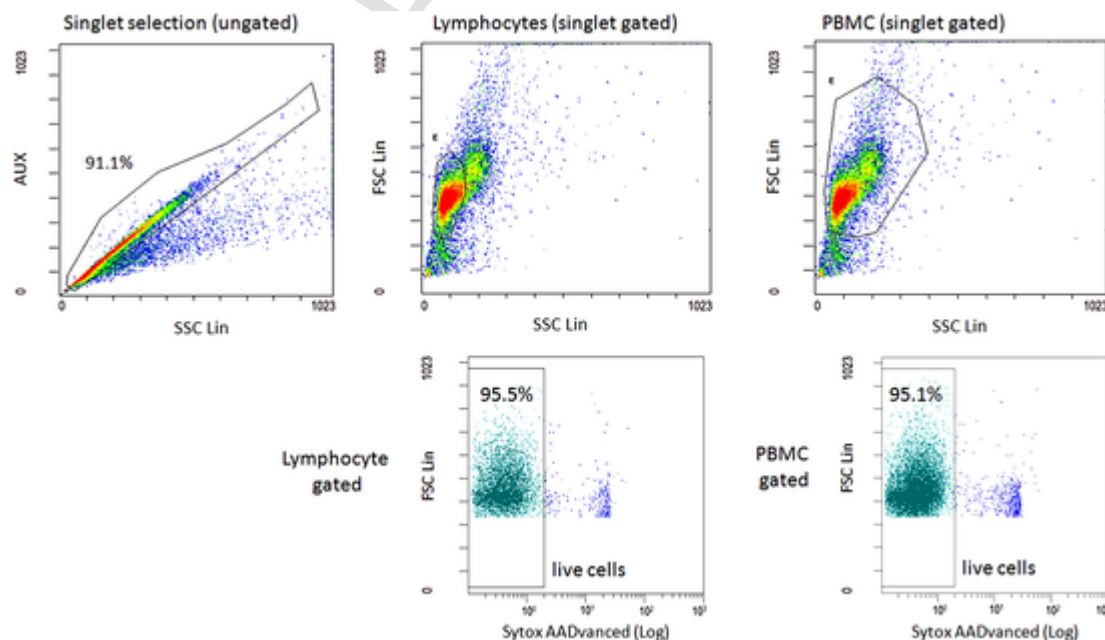
Fig. 1. Gating strategy for flow cytometry analysis of porcine circulating lymphocytes and PBMC upon stimulation with the killer peptide (KP). Cells were gated for singlets, and then for lymphocytes or the whole PBMC subpopulation depending on whether the analysis was focused on lymphocytes or monocytes, respectively. Dead cells were excluded by selecting low Sytox AADvanced fluorescent cells. Analysis was performed after acquisition of at least 40 000 live cells.

Table 3

PRRSV and PCV2 recall antigen features. Information regarding the type and amount of viruses used as recall antigen for stimulation of 4×10^5 PBMC in ELISPOT.

Virus strain designation	Virus type	Commercial designation	Antigen type	Ex vivo recall amount (MOI)
DV	PRRSV-1 vaccine	Porcilis® PRRS	Modified-live virus	1
VP-046-BIS	PRRSV-1 vaccine	Unistrain® PRRS	Modified-live virus	1
BS/114/S	PRRSV-1 field isolate	–	Live virus	1
BS/55	PRRSV-1 field isolate	–	Live virus	1
I12/11-10K15	PCV2b field isolate	–	Live virus	0.1
Bakker-11D26	PCV2b field isolate	–	Live virus	0.1

3.2. Modulation of monocyte and lymphocyte subsets in PBMC

The effect of KP was tested in vitro on PBMC by evaluating phenotype changes of innate and adaptive immune cells. The percentages of monocytes, identified as $CD172\alpha^+CD14^+$ cells, were remarkably modulated from 1 h onwards. The cell subpopulation displayed a significant increase of the $CD14^{+high}$ fraction and a corresponding decrease of the $CD14^{+low}$ fraction. A significant inversion ($p < 0.05$) of these two subsets was demonstrated upon stimulation with 20–40 μg/mL KP during incubation for up to 20 h (Fig. 2).

KP induced a gradual increase of the $CD3^+CD16^+$ NKT cell subset beginning at 1 h. The reduction of the $CD3^-CD16^+$ NK cell counterpart was observed from 4 h at 40 μg/mL (Fig. 3). KP had an early and strong activation effect on both $CD14^+$ monocytes and $CD3^+CD16^+$ NKT cells in terms of phenotypic and functional modulation by inducing CD14 and CD3 expression over time, respectively.

$CD3^+CD8\alpha^+$ and $CD3^+CD4^+$ lymphocyte percentages were significantly increased in a KP dose-dependent manner at 20 h ($p < 0.05$, data not shown). Analysis of the proportion of CD4/CD8α T cell subsets showed that DP $CD4^+CD8\alpha^+$ T cells increased markedly depending on KP concentration, from 10 to 30 % on average ($p < 0.05$) at 20 h, while naïve $CD4^+CD8\alpha^-$ Th lymphocytes did not show significant changes at any time point (Fig. 4).

It is worth noting that, in the DP $CD4^+CD8\alpha^+$ subset at 20 h post-treatment, the $CD4^+CD8\alpha^{+low}$ fraction slightly increased depending on KP concentration while the $CD4^+CD8\alpha^{+high}$ fraction, which was negligible in unstimulated cells and for up to 4 h, showed a strong KP dose-dependent increase (Fig. 4). KP remarkably modulated $CD3^+$ T lymphocytes by inducing CD4 and CD8α surface expression. For DP memory T cells in particular, KP induced the expression of high levels of CD8α, which was consistent with a cytotoxic/cytolytic phenotype.

$CD3^+$ T cells expressing CD8β as well as $CD4^-CD8\alpha^{+high}$ $CD8\beta^+$, indicative of "classical" CTL, displayed a significant dose-dependent increase from 10 % to 45–50 % at 20 h ($p < 0.05$, data not shown). As expected, $CD4^+CD8\alpha^+$ cells in unstimulated samples and in briefly-stimulated samples were $CD8\beta^-$. Of note, CD8β expression was significantly detected upon stimulation for 20 h with 20 and 40 μg/mL KP. Specifically, CD4+ cells expressing high levels of CD8α ($CD4^+CD8\alpha^{+high}$) co-expressing CD8β were increased to a greater extent compared to $CD4^+CD8\alpha^{+low}CD8\beta^+$ ($p < 0.05$, Fig. 5A). CD8β positivity was also modulated as mean fluorescence intensity (MFI) in both $CD4^+CD8\alpha^{+low}$ and $CD4^+CD8\alpha^{+high}$ cells at 20-h post-incubation (Fig. 5B). Particularly, CD8β on $CD4^+CD8\alpha^{+high}$ cells was modulated from lower to higher expression ($CD8\beta^{+low}$ to $CD8\beta^{+high}$) in a dose-dependent manner (Fig. 5B, C). KP induced CD8β expression during 20 h on "classical" CTL and also on DP $CD4^+CD8\alpha^+$ memory T cells, especially on cells expressing another marker of cytotoxicity, $CD8\alpha^{+high}$

, which thus acquired a DP CTL phenotype. In addition, the differential CD8β expression on $CD4^+CD8\alpha^{+high}$ cells indicated a further plasticity of this subset.

3.3. ELISA quantification of cytokine release in PBMC supernatants

Quantification of cytokine release in supernatants of KP-stimulated PBMC showed that the peptide induced low levels of IFN-α and high levels of TNF-α ($p < 0.05$). No significant differences were observed for the different KP doses at each time point. KP induced considerable dose- and time-dependent increases of the IFN-γ levels ($p < 0.05$). The levels of IL-10 were highly variable and were not significantly dependent on either KP dose or incubation time (Fig. 6).

The induction of IFN-α, TNF-α, and in particular the time-dependent increase of IFN-γ upon KP stimulation supported the potential of the peptide of triggering and sustaining a Th1 immune response.

3.4. ELISPOT quantification of PRRSV- and PCV2-specific IFN-γ SC frequencies and single cell IFN-γ productivity

The effect of KP was evaluated on the anti-viral immune response in PBMC of PRRSV- and PCV2-vaccinated pigs in terms of frequencies of circulating antigen-specific IFN-γ SC recalled by PRRSV and PCV2 alone and following simulataneous (KP + virus) ex vivo stimulation or a sequential in vitro pre-stimulation with KP followed by incubation with each virus (Fig. 7).

The 20-h stimulation with each PRRSV vaccine strain and each field isolate showed average responses between 65 and 125 IFN-γ SC/10⁶ PBMC. Stimulation with each PCV2 field isolate showed average responses between 105 and 115 IFN-γ SC/10⁶ PBMC. Unvaccinated pigs tested negative for virus-specific IFN-γ SC. The responses were comparable with those in unstimulated cells and showed comparable spot frequencies when PBMC were stimulated with KP (data not shown). In vaccinated pigs, the addition of KP induced significant increases of virus-specific responses at all concentrations, with 10 μg/mL KP inducing the strongest response ($p < 0.05$). Slightly lower stimulation was observed with 20-h KP pre-stimulation and subsequent stimulation with each PRRS virus compared to the simultaneous stimulation (KP + virus). However, the incremental responses were comparable among viruses. Shortening KP pre-stimulation to 4 h yielded significantly higher recall responses by PRRSV vaccine strains compared to those induced by the field isolates ($p < 0.05$). Further reduction of pre-stimulation to 1 h and 20 min led to extremely low responses. These results are presented in Fig. 7, shown in terms of differential increase (Δ) of IFN-γ SC frequencies.

The 20-h ex vivo recall responses to PCV2 were increased when KP was added and were comparable between the two isolates. However, pre-stimulation conditions produced lower responses as observed with PRRSV (Fig. 7).

Ex vivo simultaneous stimulation for 20 h with PRRSV or PCV2 and KP was the most efficient stimulation condition in which the synergistic effect of KP in inducing a higher frequency of virus-specific SC was observed. Such an increase may be related to the stimulation and augmented functions of both APC and T cells activated to secrete IFN-γ.

The ELISPOT results analyzed as percentage increase (Table 4) revealed the most remarkable variations upon ex vivo 20-h recall and 20-h pre-stimulation ($p < 0.05$). In addition to the increased IFN-γ SC frequencies when cells were co-stimulated with viruses and KP, visual analysis of IFN-γ spots detected increased single cell productivity, especially concerning PRRS viruses (Fig. 8).

The response increase, ranging from 30 % to 50 % for PRRSV-stimulated cells compared to approximately 15 % for PCV2-stimulated cells, and the increase in the secretion potential (amount of IFN-γ secreted by a single cell) suggest that a strong effect was preferentially induced when RNA strains were used as recall antigens, despite being derived from the same PRRS virus type 1 prototype.
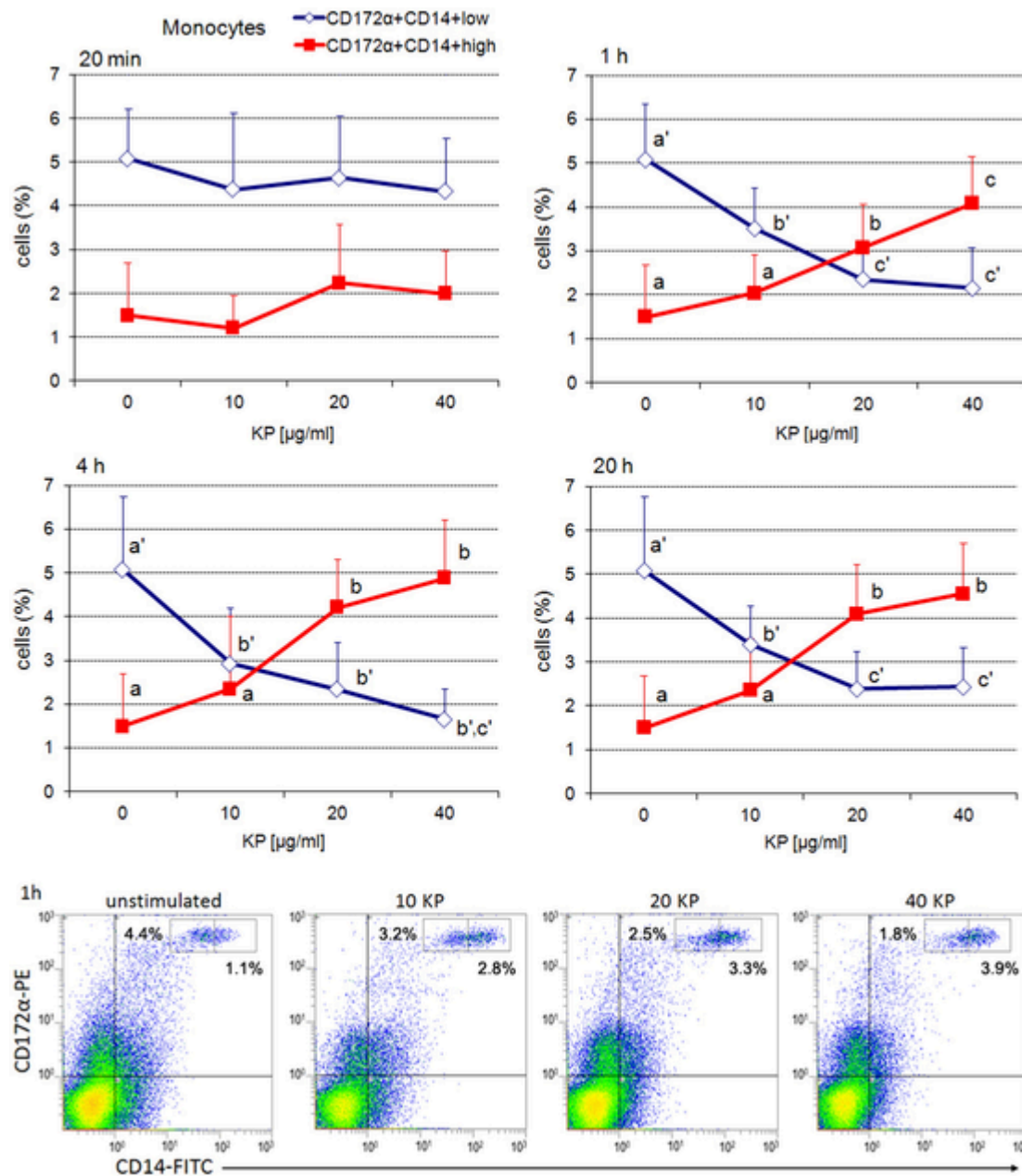
Fig. 2. Phenotypic shift of CD172α^+CD14$^+$ monocytes in response to KP. Percentage values are reported based on CD14$^{+\,low}$ and CD14$^{+\,high}$ surface expression in PBMC upon stimulation for 20 h with 0, 10, 20, or 40 μg/mL KP or for the last 4 h, 1 h, and 20 min. Data are expressed as mean values ± standard deviation (SD). Different letters indicate significant differences between the responses at different concentrations in the cell subset (p < 0.05). The results are representative of two independent experiments. The representative density plots show activation of KP-stimulated cells at 1 h compared to unstimulated cells in terms of dose-dependent shift from a majority of CD172α + CD14 + ^{low} cells to a prevalence of CD172α + CD14 + ^{high} cells. For color figure information, please refer to the online manuscript.

Stimulation with KP alone produced comparable or sligltly higher responses than those in unstimulated cells. Stimulation of PBMC with impaired viability was included to determine whether the KP dose-dependent response reduction was due to cell death during the ELISPOT assay. Cell viability after 20-h incubation was not significantly affected by KP and KP + virus treatments. Consequently, no evidence of cell death in terms of DNA release was observed, except for the cell death positive controls (Fig. 8).

In-depth analysis of spot features highlighted fuzzy blurred spots ("spot shadows") at 20 μg/mL, and more markedly at 40 μg/mL KP. Therefore, these conditions were excluded from quantification due to altered spot size and gradient, and/or extremely reduced intensity (Fig. 9). These results support a hypothetical interference phenomenon by

KP in spot formation likely due to self-assembled KP aggregates between the cell suspension and the anti-IFN-γ coating Abs, and a potentially different sedimentation kinetics between PBMC and KP aggregates in the well.

4. Discussion

The early immunomodulatory effects of an engineered antibody-based killer peptide (KP) obtained using the anti-idiotypic approach were investigated in swine PBMC. KP is the engineered result of the internal image of a yeast killer toxin selected to be safe and used for in vitro and in vivo studies. Cytotoxicity was demonstrated to be absent even at high concentrations [11,13]. The lymphoproliferation/cytotoxicity assay results of this study confirmed that KP concentrations up
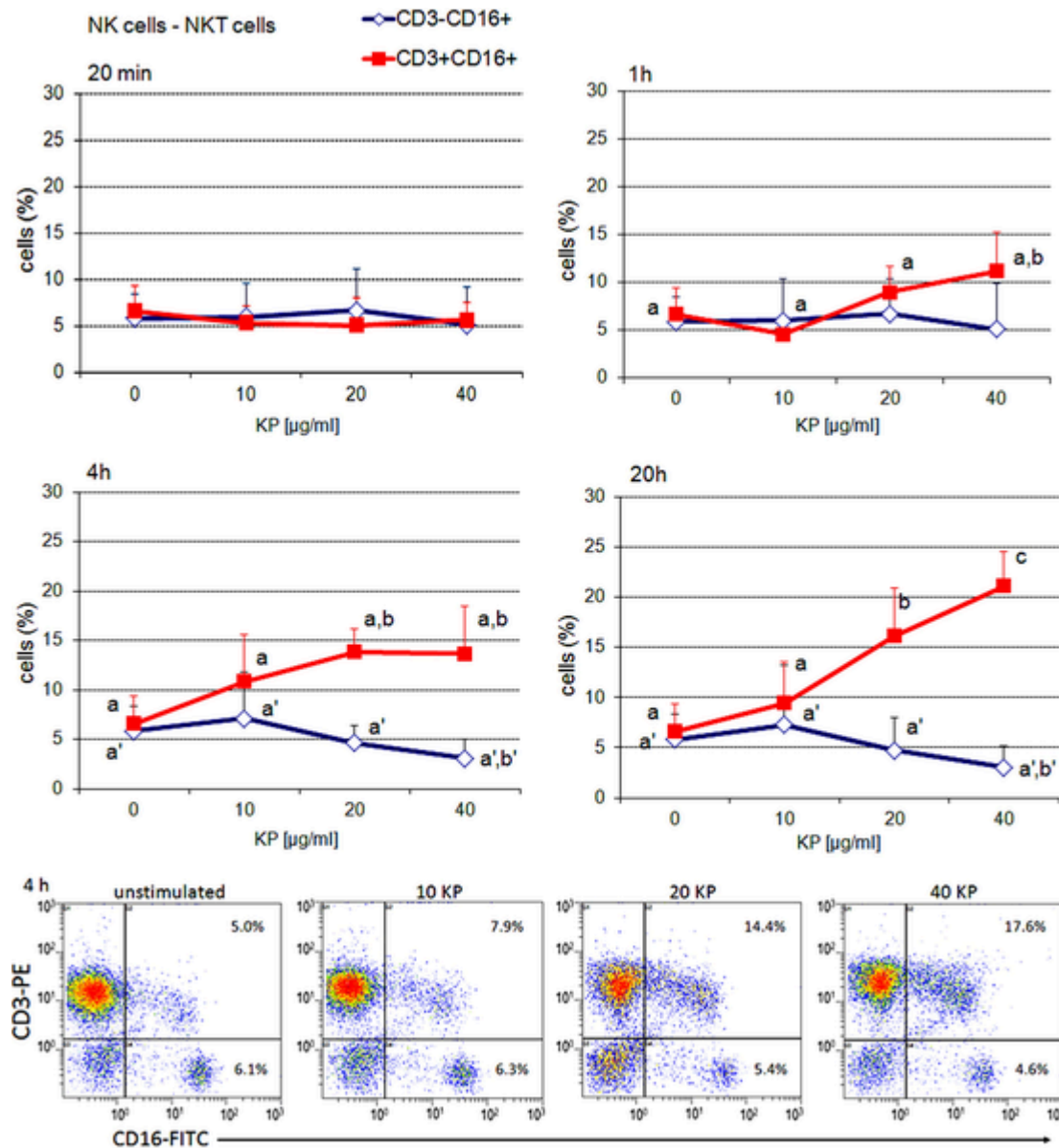
Fig. 3. KP induced modulation of CD16$^+$ cell subsets within lymphocytes. The percentage levels of lymphocyte-gated CD3$^+$CD16$^+$ and CD3$^-$CD16$^+$ subsets in PBMC upon stimulation for 20 h with 0, 10, 20, or 40 μg/mL KP or for the last 4 h, 1 h, and 20 min. are shown. Data are expressed as mean values ± standard deviation (SD). Different letters indicate significant differences between responses at different concentrations in the cell subset (p < 0.05). The representative density plots show NK and NKT cell modulation after stimulation with KP for 4 h compared to unstimulated cells. The results are representative of two independent experiments. For color figure information, please refer to the online manuscript.

to 40 μg/mL did not induce either replication/increased metabolic activity or cytotoxicity in porcine PBMC.

Incubation with KP from 20 min to 20 h showed that the peptide strongly modulates the phenotype of CD172α$^+$CD14$^+$ monocytes, triggering a dose-dependent up-regulation of CD14 (CD14^{+high}) and the acquisition of a pro-inflammatory phenotype [21,43,44].

These results confirm what was previously observed upon a longer exposure time [37] and suggest how CD14$^+$ monocytes can be promptly activated by KP [45] and are likely responsible for TNF-α secretion in culture supernatants.

TNF-α induction was also observed upon stimulation with other Ab-derived molecules, namely VHCDR3 and N10 K, which can modulate immune cells by triggering cytokine release during comparable KP incubation times, starting from 30 min to 1 h [46,47]. In a murine model, it was demonstrated that KP is preferentially taken up by cells of the monocyte-macrophage lineage [14], which are potent TNF-α producers.

In the present study, pronounced dose- and time-dependent increases of lymphocytes expressing CD16 were evident owing to the increase of the CD3$^+$CD16$^+$ NKT cell subset. NKT cells can be rapidly activated and secrete pro-inflammatory cytokines such as IL-6, as well as IFN-γ [24–26,48]. Therefore, these early activated cells may be involved in the IFN-γ secretion that was observed in this study and require further investigation.

The dose-dependent increase of both CD3$^+$CD4$^+$ and CD3$^+$CD8α$^+$ cells, and the increased expression of CD8α on T cell subsets was due to the marked increase of DP CD4$^+$CD8α$^+$ Th memory cells. While this subset has been shown to be comprised of CD4$^+$CD8α^{+low} cells [27,28,34], incubation with the highest dose of KP resulted in a notable increase of DP cells expressing high levels of CD8α (CD8α^{+high}) at 20 h.

Moreover, the increase of CD3$^+$CD8β$^+$ cells, commonly composed of cells with cytolytic/cytotoxic functions ("classical" CTL) [19], was also due to a fraction of DP cells expressing CD8β at KP concentra-
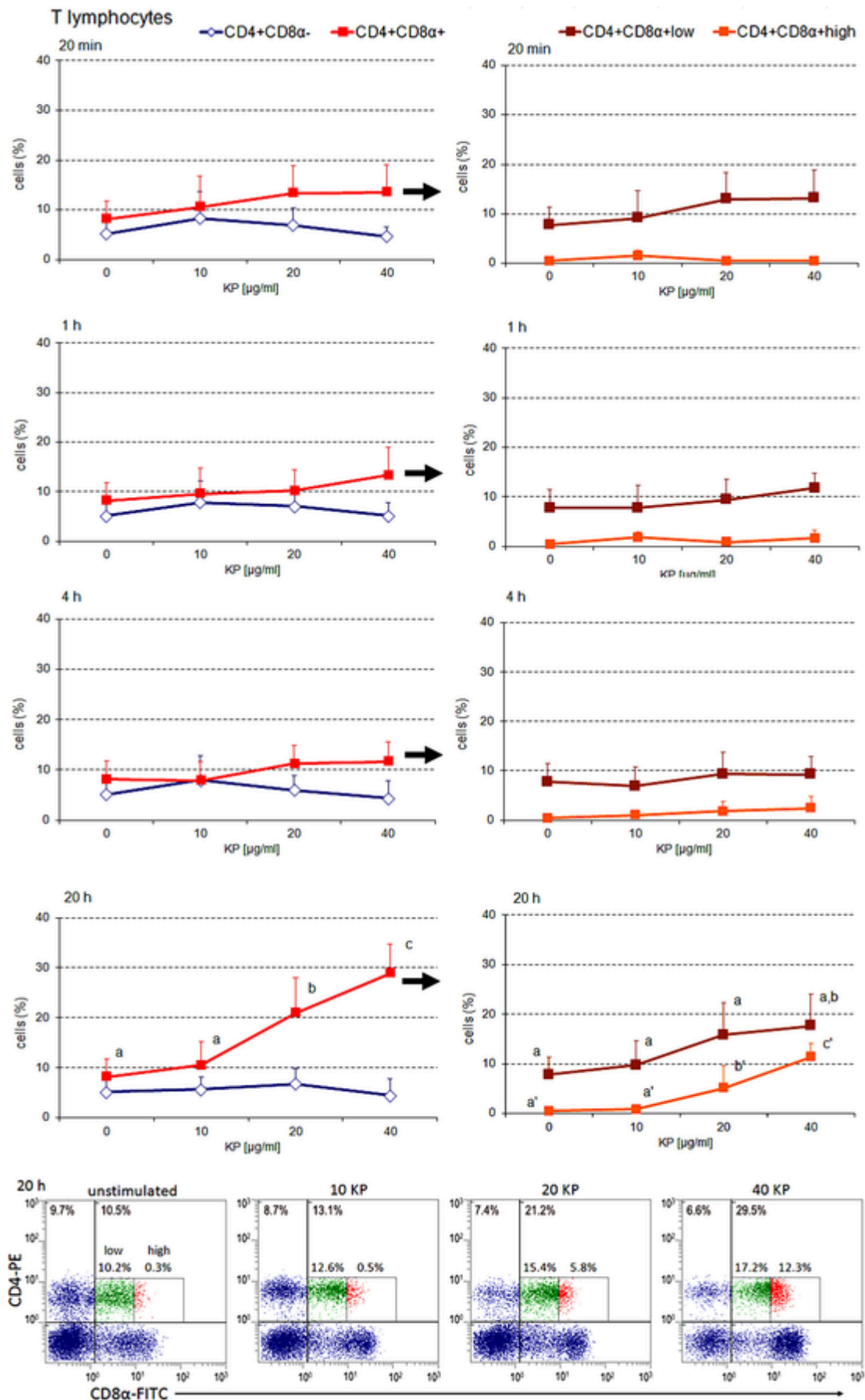
Fig. 4.

Stimulation of blood CD4$^+$CD8α$^+$ T lymphocytes by KP. The percentage levels of CD4$^+$CD8α$^-$ and CD4$^+$CD8α$^+$ cells in PBMC upon stimulation for 20 h with 0, 10, 20, or 40 μg/mL KP or for the last 4 h, 1 h, and 20 min are shown. In the right column, graphs show the fractions of CD4$^+$CD8a^{+low} and CD4$^+$CD8a^{+high} within the CD4$^+$CD8a$^+$ subset. The representative density plots show T cell activation in terms of increase of the two CD4$^+$CD8α$^+$ subsets upon 20 h KP stimulation compared to unstimulated cells. Data are expressed as mean values ± standard deviation (SD). Different letters indicate significant differences between the responses at different concentrations in the cell subset (p < 0.05). The results are representative of two independent experiments. For color figure information, please refer to the online manuscript.

tions of 20 and 40 μg/mL at 20 h. This subset was detectable upon stimulation, especially in the DP CD4$^+$CD8α^{+high} cell fraction, and increased differently in CD4$^+$CD8α^{+high} and CD4$^+$CD8α^{+low} cells, suggesting differential responsiveness of these two latter subsets.

The strong up-regulation of CD8β expression (MFI) observed only on DP CD4$^+$CD8α^{+high} T lymphocytes suggests the existence of at least two distinct subsets following stimulation/activation (CD4$^+$CD8α^{+low}CD8β^{+low} and CD4$^+$CD8α^{+high}CD8β^{+high}) which warrants further investigation. In humans, differential CD8β expression was observed, leading to the identification of a CD8β^{+low} and a CD8β^{+high} subset [49].

The modulation of CD8β$^+$ cells can be evaluated considering that, like humans, pigs also have several known or potential isoforms of the CD8B gene (coding for the CD8β protein) due to alternative splicing. In humans, there are four CD8B gene splice variants (M1 to M4) and these isoforms are differently expressed by different T cell subsets [50,51]. In particular, surface expression of the M2 isoform is strongly influenced by in vitro stimulation. It was observed that M2 CD8β protein localization to the cell surface increased during short-term stimulation (from 1 to 6 h), together with the CD3 protein [51].

In our conditions, KP induced an increased percentage of CD8β$^+$ cells and also increased MFI at 20-h post-stimulation. Therefore, in pigs the course of CD8β surface expression and thus the increase of the CD8β$^+$ cell fractions can potentially be explained by the involvement of a specific CD8β variant in the functions of CD8$^+$ T cells.

It has been proposed that such isoforms in humans most likely influence coreceptor-mediated signaling and influence the extent and duration of the immune response.

The DP phenotype, which is usually evident after acquisition of CD8α expression, may also have been acquired following expression of CD4 on CD8α^{+high} lymphocytes upon activation [20,52].

Overall, the immunomodulation leading to increased fractions of NKT cells, memory Th lymphocytes, classical CTL and DP CTL, and possibly CD3$^+$CD8$^+$CD16$^+$ lymphokine-activated killer (LAK) cells could be responsible for the dose- and time-dependent increases of IFN-γ release in culture supernatants [22,53]. In this view, the results highlight how the effects induced by KP can support a marked Th1 response.

KP was also tested for its potential in modulating the antigen-specific response to two major pig viruses, PRRSV and PCV2. IFN-γ ELISPOT results demonstrated that KP can trigger the response to these viruses and may be able to increase the sensitivity of the assay. Previous studies evaluating the addition of potential adjuvants, such as cytokines (IL-15, IL-7, IL-15 + IL7, IFN-α) and anti-CD28 Ab to amplify the sensitivity and specificity of ELISPOT (thus termed AMPLISPOT) in measuring low frequency virus-specific (HIV, HCV) cells in blood from humans and pigs (PRRSV) have reported discordant results [54–58].

In our study, the effects of KP on PRRSV-specific and PCV2-specific IFN-γ responses included both increased cell frequencies and increased IFN-γ productivity in single cells, compared to cells stimulated only with virus (synergistic effect). This effect may be due to the ability of KP to positively modulate innate immune cells, such as monocytes and dendritic cells (DC), which can act as antigen presenting cells (APC) that lower the activation threshold of CD4$^+$ memory T cells and effector CD8$^+$ T cells, whose functional avidity for antigen depends on their activation status [59–61]. On the other hand, the effect may be due to a stimulatory effect on memory T cells in terms of activation and increased IFN-γ secretion.

The same results were observed in PBMC recalled by both vaccines and heterologous virus isolates, suggesting that recalled memory T cells are characterized by cross-reactivity. This effect seemed to be more pronounced upon PRRSV-1 co-stimulation (KP + virus) than upon PCV2 co-stimulation, suggesting that KP has a potent effect on PRRSV, an RNA virus, as demonstrated against other RNA viruses, including HIV and influenza A viruses in humans, in which polyfunctional cross-reactive cells play a major role in immune defense [11,12,62,63].

The dose-dependent decrease of the ELISPOT response in PRRSV- and PCV2-stimulated cells is attributed to the ex vivo interference effect due to the self-assembling formation of KP aggregates [15–18]. The sedimentation kinetics and/or the presence of KP itself may have interfered with spot formation at the highest concentrations. Short-term KP pre-incubation (from 20 min to 4 h) induced a much lower synergistic effect in response to the two viruses, compared to the other conditions (20-h stimulation), which was likely due to the suboptimal stimulation of antigen-specific IFN-γ SC.

This likely explains why, even though significant increases of IFN-γ SC were detected at all KP concentrations, the responses did not follow the same dose-dependent increase of the IFN-γ release in ELISA, or of the cells responsible for IFN-γ secretion in FCM. Other effects and artifacts due to ex vivo incubation were carefully evaluated and excluded based on previous studies [33,38] and ELISPOT validated guidelines [64,65].

Overall, KP early modulated several immune cells displaying cytokine release and innate inflammatory and cytotoxic effector functions as well as cells responsible for immune memory surveillance. Importantly, such T cell subsets also share a cytolytic/cytotoxic phenotype, being CD4$^+$CD8α^{+low} β^{+low} or CD4$^+$CD8α^{+high} β$^{+low/+high}$, and can play an important role during various Th1 multifunctional responses to infections. Furthermore, the augmented IFN-γ responsiveness observed in PRRSV-1- and PCV2b-primed cells suggests the potential of KP as immunostimulant and/or vaccine adjuvant.

Ethics approval

Sample collection from pigs used in the study was carried out following ethics and good clinical practice (GCP) guidelines in animal treatment and welfare.

Declaration of Competing Interest

None.

### Authors' contributions

LF, PB, PM and WM contributed to the conceptualization and methodology of the study. LF, GF, GB and GO carried out assays and analyses; LF, PB, EDA contributed to analyses and data interpretation and curation; LF wrote the manuscript. LF, PB, EDA, RS, BP and VC provided review and editing of the manuscript. All authors read and approved the manuscript.

Acknowledgements
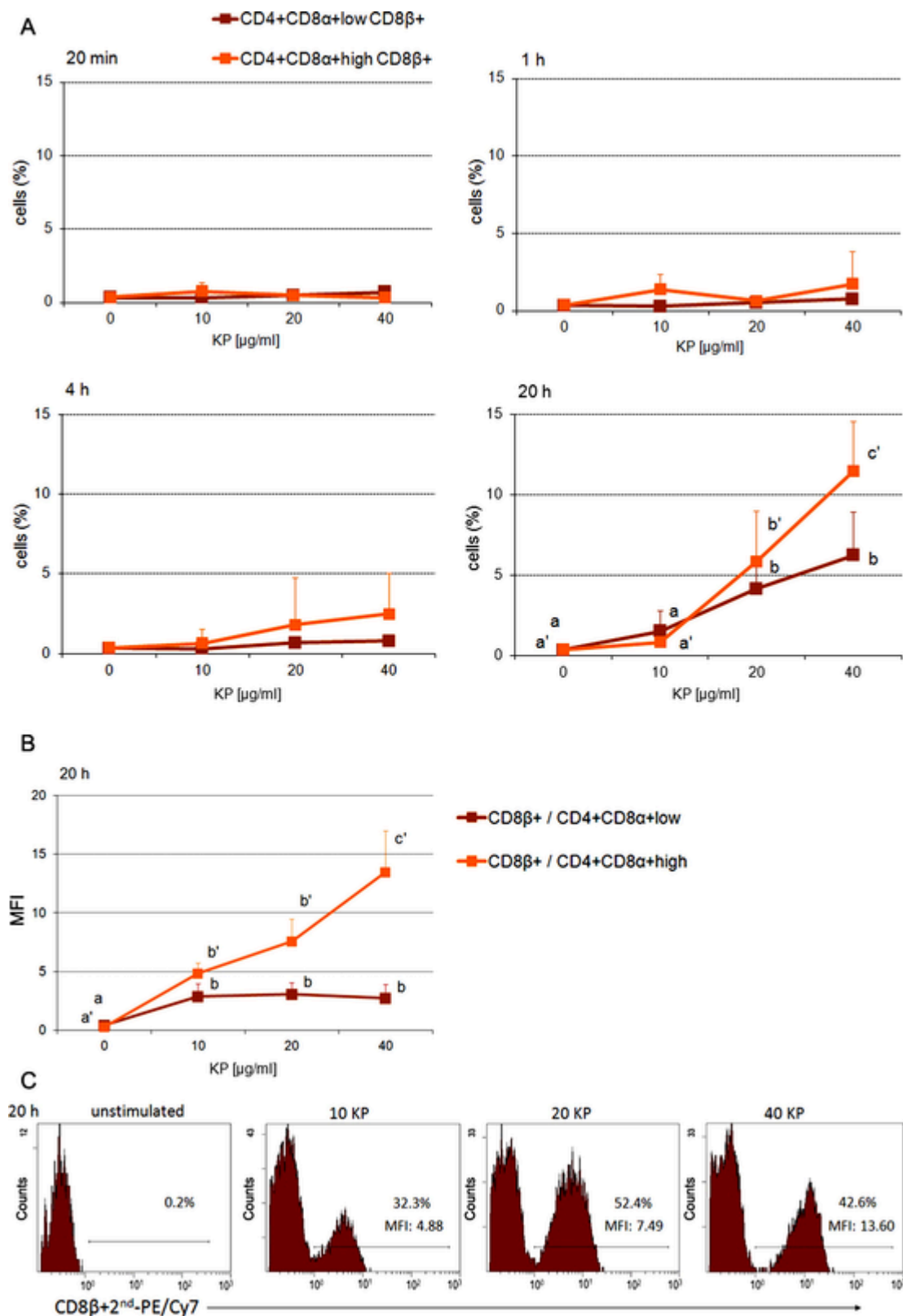
Fig. 5. Induction of CD8β surface expression on blood CD4$^+$CD8α$^+$ T lymphocytes by KP. A) The percentage levels of CD4$^+$CD8α^{+low}β$^+$ cells and CD4$^+$CD8α^{+high}β$^+$ cells in PBMC upon stimulation for 20 h with 0, 10, 20, or 40 μg/mL KP or for the last 4 h, 1 h, and 20 min are shown. B) Surface expression modulation in terms of mean fluorescence intensity (MFI) of CD8β$^+$ (CD8β$+^{low}$ and CD8β$+^{high}$) cells within the CD4$^+$CD8α^{+low} and the CD4$^+$CD8α^{+high} cell fractions upon 20 h stimulation. C) Representative histogram plots of CD8β$^+$ cells showing the increase of MFI. Data are expressed as mean values ± standard deviation (SD). Different letters indicate significant differences between the responses in the cell subset at different concentrations (p < 0.05). The results are representative of two independent experiments. For color figure information, please refer to the online manuscript.
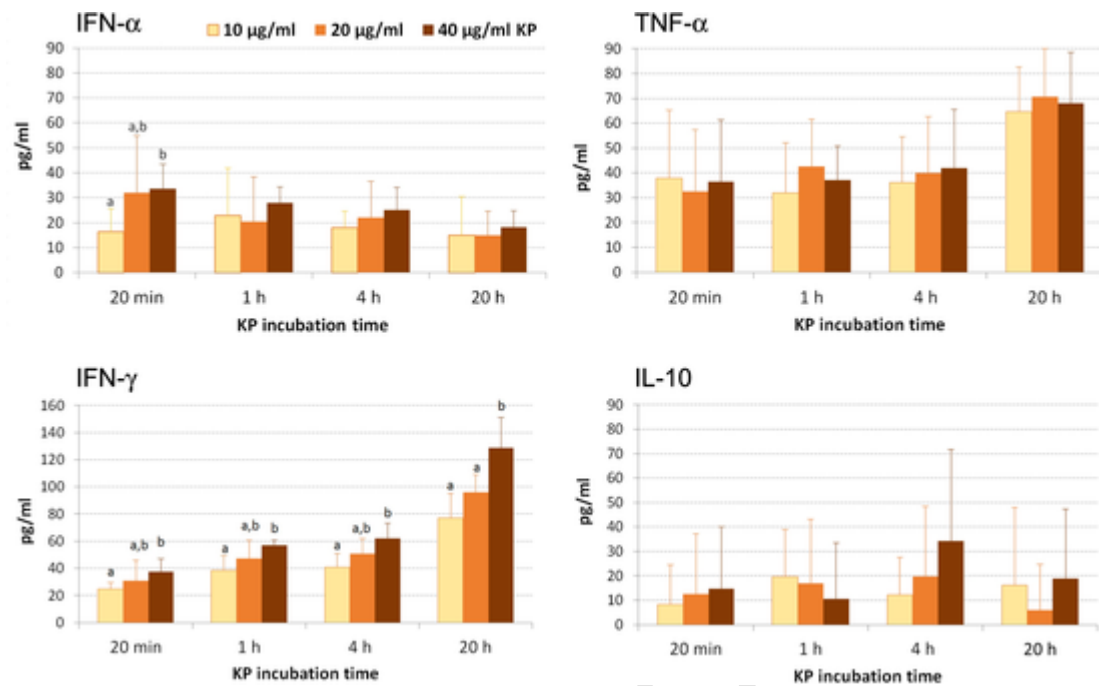
Fig. 6. Secretion of IFN-α, TNF-α, IFN-γ, and IL-10 in supernatants of KP-stimulated PBMC. Cells were stimulated for 20 h with 0, 10, 20, or 40 µg/mL KP or for the last 4 h, 1 h, and 20 min. Cytokine release was quantified by sandwich ELISA and is reported after subtraction of the relative values in unstimulated cells. Data are expressed as mean values ± standard deviation (SD). Different letters indicate significant differences between the responses at different KP concentrations (p < 0.05). The results are representative of two independent experiments.

Fig. 7. Synergistic effect of KP on PRRSV- and PCV2-specific IFN-γ secreting cell frequencies in PBMC of PRRSV- and PCV2-vaccinated pigs. The graphs show the differential increase (delta, Δ) of IFN-γ SC in PRRSV + KP or PCV2 + KP stimulated samples (4 × 10^5 PBMC) calculated by subtraction of the corresponding PRRSV alone or PCV2 alone stimulated samples and the KP alone stimulated samples, normalized to 10^6 PBMC. The value in unstimulated cells (negative control) was subtracted from each value for each stimulation condition. For proper comparisons, only data relative to stimulation with 10 μg/mL KP are reported because of the interference effect observed at 20 and 40 μg/mL KP (see text and Figs. 8 and 9 for details). 20 h ex vivo: stimulation for 20 h with each virus and KP; 20 min pre-stim, 1 h pre-stim, 4 pre-stim, 20 h pre-stim: pre-stimulation of PBMC with KP for the indicated times followed by stimulation with each virus for 20 h. The viral antigens used for stimulation were: PRRSV-1 DV: vaccine strain; PRRSV-1 VP: vaccine strain; PRRSV-1 BS/114/S: field isolate; PRRSV-1 BS/55: field isolate; PCV2b I12/11: field isolate; PCV2b Bakker: field isolate; pre-stim: KP pre-stimulation. Different letters indicate significant differences between the responses at different incubation time-points. Data are expressed as mean values ± standard deviation (SD). The results are representative of two independent experiments. For color figure information, please refer to the online manuscript.
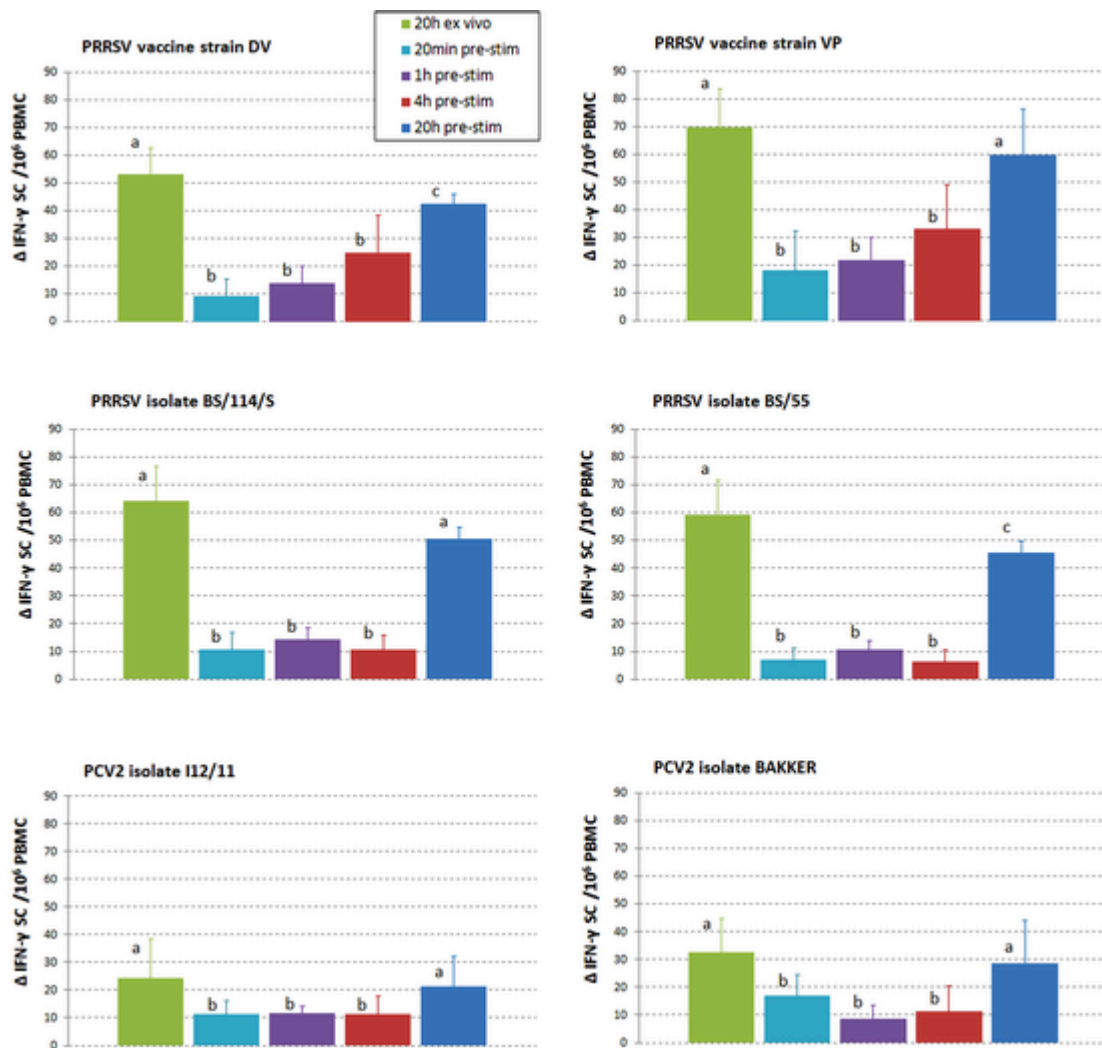
Table 4

Percentage increase of virus-specific IFN-γ SC frequencies in PBMC simultaneously stimulated with PRRSV + KP or PCV2 + KP. The data show the percentage increase calculated by dividing the differential increase (delta value, Δ) defined in Fig. 7 by the value in PRRSV + KP or PCV2 + KP stimulated cells, and multiplying by 100. Only data relative to stimulation with 10 μg/mL KP are reported because of the interference effect at 20 and 40 μg/mL KP (see text and Figs. 8 and 9 for details). Data are expressed as mean values ± standard deviation (SD). The results are representative of two independent experiments. PRRSV-1 DV: vaccine strain; PRRSV-1 VP: vaccine strain; PRRSV-1 BS/114/S: field isolate; PRRSV-1 BS/55: field isolate; PCV2b I12/11: field isolate; PCV2b Bakker: field isolate. 20 h ex vivo: stimulation for 20 h with PRRSV + KP or PCV2 + KP directly in ELISPOT plates; Pre-stim: KP pre-stimulation condition before incubating pre-stimulated PBMC with each virus in ELISPOT plates.

Percentage increase (%) in virus-specific IFN-γ secreting cell frequencies

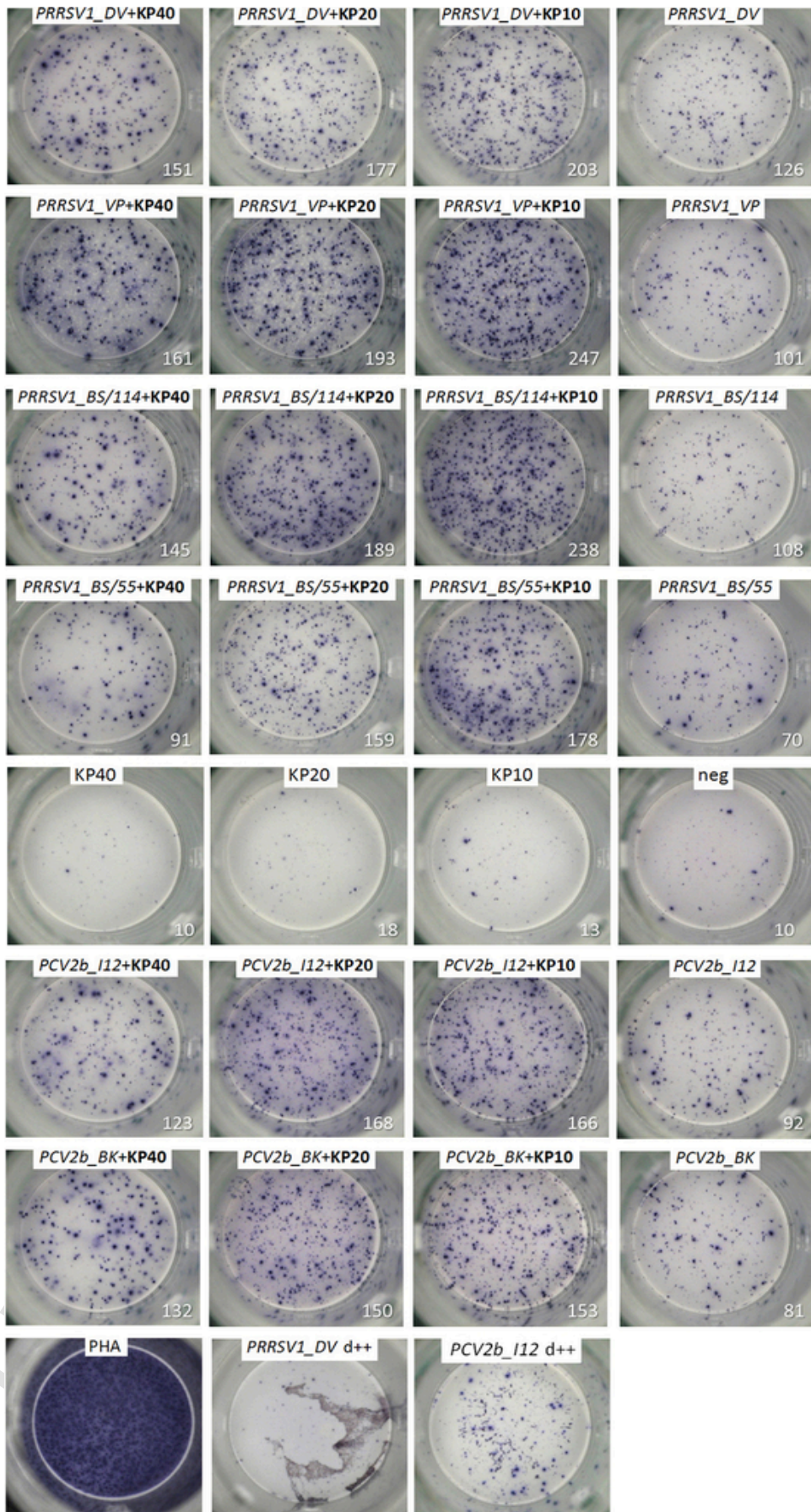| + KP (10 μg/mL)		PRRSV-1 DV	PRRSV-1 VP	PRRSV-1 BS/114/	PRRSV-1 BS/55	PCV2b I12/11	PCV2b Bakker
20 h ex vivo	Mean	30	35	41	46	14	13
	SD	8	5	10	13	10	9
Pre-stim 20 h	Mean	31	33	34	38	16	14
	SD	3	13	3	4	9	10
Pre-stim 4 h	Mean	19	22	9	7	11	10
	SD	11	14	5	6	8	8
Pre-stim 1 h	Mean	12	15	12	12	10	7
	SD	7	6	5	5	5	5
Pre-stim 20 min	Mean	8	10	9	8	7	11
	SD	3	6	6	6	6	9

Fig. 8.

Boosting effect of KP on PRRSV- and PCV2-specific IFN-γ secreting cell frequencies and single cell IFN-γ productivity (single cell secretion). Representative responses in PBMC of PRRSV- and PCV2-vaccinated pigs and dose-dependent (μg/mL) effect of ex vivo incubation with PRRSV or PCV2 strains and different KP concentrations (10, 20, and 40 μg/mL). Stimulation was carried out in cRPMI-1640 for 20 h with PRRSV-1 DV MLV vaccine strain (1 MOI), PRRSV-1 VP-046-BIS MLV vaccine strain (1 MOI), PRRSV-1 BS/114/S and BS/55 field isolates (1 MOI), and PCV2b I11/12-10K15 and PCV2b Bakker-11D26 field isolates (0.1 MOI). The numbers are relative to the spots counted in the stimulated well (4×10^5 PBMC). The results are representative of two independent experiments. Cells stimulated with KP alone and unstimulated cells are shown. A positive reactivity control (5 μg/mL PHA) and a cell death positive control (d + +) of PRRSV- and PCV2-stimulated PBMC (subjected to improper freezing-thawing) are shown to exclude cell death effects (DNA release) from that observed at 40 μg/mL KP. For color figure information, please refer to the online manuscript.

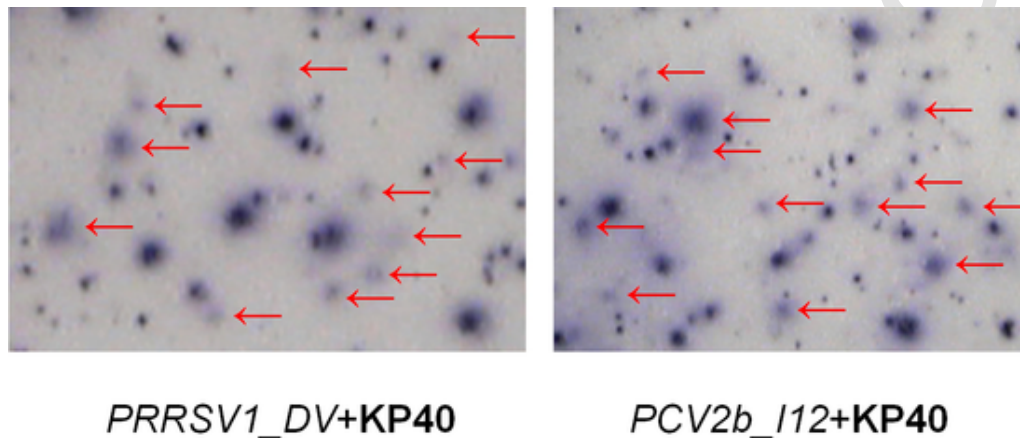*PRRSV1_DV+***KP40**   *PCV2b_I12+***KP40**

Fig. 9. Interference phenomenon by KP in ELISPOT spot formation. The two magnified micrographs highlight selected areas of the two representative wells PRRSV1_DV + KP40 and PCV2b_I12 + KP40 shown in Fig. 8 (20-h ex vivo stimulation). Interference is evident as fuzzy blurred spots or "spot shadows". These were excluded from quantification due to altered spot size and gradient, and/or extremely reduced intensity (red arrows). For color figure information, please refer to the online manuscript.

References

[1] S Patel, N Akhtar, Antimicrobial peptides (AMPs): the quintessential 'offense and defense' molecules are more than antimicrobials, Biomed. Pharmacother. 95 (2017) 1276–1283, doi:10.1016/j.biopha.2017.09.042.

[2] A M Blom, Strategies developed by bacteria and virus for protection from the human complement system, Scand. J. Clin. Lab. Invest. 64 (2004) 479–496, doi:10.1080/00365510410002904.

[3] T Ciociola, W Magliani, L Giovati, M Sperindé, C Santinoli, G Conti, S Conti, L Polonelli, Antibodies as an unlimited source of anti-infective, anti-tumour and immunomodulatory peptides, Sci. Prog. (New Haven) 97 (2014) 215–233, doi:10.3184/003685014x14049273183515.

[4] T Ciociola, L Giovati, M Sperindè, W Magliani, C Santinoli, G Conti, S Conti, L Polonelli, Peptides from the inside of the antibodies are active against infectious agents and tumours, J. Pept. Sci. 21 (2015) 370–378, doi:10.1002/psc.2748.

[5] T Ciociola, L Giovati, S Conti, W Magliani, C Santinoli, L Polonelli, Natural and synthetic peptides with antifungal activity, Future Med. Chem. 8 (2016) 1413–1433, doi:10.4155/fmc-2016-0035.

[6] W Magliani, S Conti, R L Cunha, L R Travassos, L Polonelli, Antibodies as crypts of antiinfective and antitumor peptides, Curr. Med. Chem. 16 (2009) 2305–2323, doi:10.2174/092986709788453104.

[7] W Magliani, S Conti, L Giovati, P P Zanello, M Sperindè, T Ciociola, L Polonelli, Antibody peptide based antifungal immunotherapy, Front. Microbiol. 3 (2012) 190, doi:10.3389/fmicb.2012.00190.

[8] W Magliani, L Giovati, T Ciociola, M Sperindè, C Santinoli, G Conti, S Conti, L Polonelli, Antibodies as a source of anti-infective peptides: an update, Future Microbiol. 10 (2015) 1163–1175, doi:10.2217/fmb.15.36.

[9] C Cafarchia, D Immediato, G D Paola, W Magliani, T Ciociola, S Conti, D Otranto, L Polonelli, In vitro and in vivo activity of a killer peptide against Malassezia pachydermatis causing otitis in dogs, Med. Mycol. 52 (2014) 350–355, doi:10.1093/mmy/myt016.

[10] L Giovati, C Santinoli, C Mangia, A Vismarra, S Belletti, T D'Adda, C Fumarola, T Ciociola, C Bacci, W Magliani, L Polonelli, S Conti, L H Kramer, Novel activity of a synthetic decapeptide against Toxoplasma gondii tachyzoites, Front. Microbiol. 9 (2018) 753, doi:10.3389/fmicb.2018.00753.

[11] C Casoli, E Pilotti, C F Perno, E Balestra, E Polverini, A Cassone, S Conti, W Magliani, L Polonelli, A killer mimotope with therapeutic activity against AIDS-related opportunistic micro-organisms inhibits ex vivo HIV-1 replication, AIDS 20 (2006) 975–980, doi:10.1097/01.aids.0000222068.14878.0d.

[12] G Conti, W Magliani, S Conti, L Nencioni, R Sgarbanti, A T Palamara, L Polonelli, Therapeutic activity of an anti-idiotypic antibody-derived killer peptide against influenza A virus experimental infection, Antimicrob. Agents Chemother. 52 (2008) 4331–4337, doi:10.1128/AAC.00506-08.

[13] A Sala, A Ardizzoni, T Ciociola, W Magliani, S Conti, E Blasi, C Cermelli, Antiviral activity of synthetic peptides derived from physiological proteins, Intervirol. 61 (2018) 166–173, doi:10.1159/000494354.

[14] E Cenci, E Pericolini, A Mencacci, S Conti, W Magliani, F Bistoni, L Polonelli, A Vecchiarelli, Modulation of phenotype and function of dendritic cells by a therapeutic synthetic killer peptide, J. Leukoc. Biol. 79 (2006) 40–45, doi:10.1189/jlb.0205113.

[15] W Magliani, S Conti, T Ciociola, L Giovati, P P Zanello, T Pertinhez, A Spisni, L Polonelli, Killer peptide: a novel paradigm of antimicrobial, antiviral and immunomodulatory auto-delivering drugs, Future Med. Chem. 3 (2011) 1209–1231, doi:10.4155/fmc.11.71.

[16] S Paulone, A Ardizzoni, A Tavanti, S Piccinelli, C Rizzato, A Lupetti, B Colombari, E Pericolini, L Polonelli, W Magliani, S Conti, B Posteraro, C Cermelli, E Blasi, S Peppoloni, The synthetic killer peptide KP impairs Candida albicans biofilm in vitro, PLoS One 12 (2017) e0181278, doi:10.1371/journal.pone.0181278.

[17] L Polonelli, W Magliani, T Ciociola, L Giovati, S Conti, From Pichia anomala killer toxin through killer antibodies to killer peptides for a comprehensive anti-infective strategy, Antonie Van Leeuwenhoek 99 (2011) 35–41, doi:10.1007/s10482-010-9496-3.

[18] T A Pertinhez, S Conti, E Ferrari, W Magliani, A Spisni, L Polonelli, Reversible self-assembly: a key feature for a new class of autodelivering therapeutic peptides, Mol. Pharm. 6 (2009) 1036–1039, doi:10.1021/mp900024z.

[19] M Sinkora, J E Butler, The ontogeny of the porcine immune system, Dev. Comp. Immunol. 33 (2009) 273–283, doi:10.1016/j.dci.2008.07.011.

[20] W Gerner, S C Talker, H C Koinig, C Sedlak, K H Mair, A Saalmüller, Phenotypic and functional differentiation of porcine αβ T cells: current knowledge and available tools, Mol. Immunol. 66 (2015) 3–13, doi:10.1016/j.molimm.2014.10.025.

[21] L Fairbairn, R Kapetanovic, D Beraldi, D P Sester, C K Tuggle, A L Archibald, D A Hume, Comparative analysis of monocyte subsets in the pig, J. Immunol. 190 (2013) 6389–6396, doi:10.4049/jimmunol.1300365.

[22] M S Denyer, T E Wileman, C M Stirling, B Zuber, H H Takamatsu, Perforin expression can define CD8 positive lymphocyte subsets in pigs allowing phenotypic and functional analysis of natural killer, cytotoxic T, natural killer T and MHC un-restricted cytotoxic T-cells, Vet. Immunol. Immunopathol. 110 (2006) 279–292, doi:10.1016/j.vetimm.2005.10.005.

[23] L Ferrari, E Canelli, E De Angelis, A Catella, G Ferrarini, G Ogno, L Bonati, R Nardini, P Borghetti, P Martelli, A highly pathogenic porcine reproductive and respiratory syndrome virus type 1 (PRRSV-1) strongly modulates cellular innate and adaptive immune subsets upon experimental infection, Vet. Microbiol. 216 (2018) 85–92, doi:10.1016/j.vetmic.2018.02.001.

[24] K H Mair, M Stadler, S C Talker, H Forberg, A K Storset, A Müllebner, J C Duvigneau, S E Hammer, A Saalmüller, W Gerner, Porcine CD3+NKp46+ lymphocytes have NK-cell characteristics and are present in increased frequencies in the lungs of influenza-infected animals, Front. Immunol. 7 (2016) 263, doi:10.3389/fimmu.2016.00263.

[25] A Thierry, A Robin, S Giraud, S Minouflet, A Barra, F Bridoux, T Hauet, G Touchard, A Herbelin, J M Gombert, Identification of invariant natural killer T cells in porcine peripheral blood, Vet. Immunol. Immunopathol. 149 (2012) 272–279, doi:10.1016/j.vetimm.2012.06.023.

[26] B L Artiaga, R L Whitener, C R Staples, J P Driver, Adjuvant effects of therapeutic glycolipids administered to a cohort of NKT cell-diverse pigs, Vet. Immunol. Immunopathol. 162 (2014) 1–13, doi:10.1016/j.vetimm.2014.09.006.

[27] A Saalmüller, T Werner, V Fachinger, T-helper cells from naive to committed, Vet. Immunol. Immunopathol. 87 (2002) 137–145, doi:10.1016/s0165-2427(02)00045-4.

[28] C Revilla, S Chamorro, B Alvarez, C Pérez, A Ezquerra, F Alonso, J Domínguez, Analysis of functional heterogeneity of porcine memory CD4 + T cells, Dev. Comp. Immunol. 29 (2005) 479–488, doi:10.1016/j.dci.2004.08.006.

[29] W Gerner, T Käser, A Saalmüller, Porcine T lymphocytes and NK cells - an update, Dev. Comp. Immunol. 33 (2009) 310–320, doi:10.1016/j.dci.2008.06.003.

[30] P Martelli, P Ardigò, L Ferrari, M Morganti, E De Angelis, P Bonilauri, A Luppi, S Guazzetti, A Caleffi, P Borghetti, Concurrent vaccinations against PCV2 and PRRSV: study on the specific immunity and clinical protection in naturally infected pigs, Vet. Microbiol. 162 (2013) 558–571, doi:10.1016/j.vetmic.2012.11.016.

[31] G Franzoni, N V Kurkure, D S Edgar, H E Everett, W Gerner, K B Bodman-Smith, H R Crooke, S P Graham, Assessment of the phenotype and functionality of porcine CD8 T cell responses following vaccination with live attenuated classical swine fever virus (CSFV) and virulent CSFV challenge, Clin. Vaccine Immunol. 20 (2013) 1604–1616, doi:10.1128/CVI.00415-13.

[32] H H Takamatsu, M S Denyer, A Lacasta, C M Stirling, J M Argilaguet, C L Netherton, C A Oura, C Martins, F Rodríguez, Cellular immunity in ASFV responses, Virus Res. 173 (2013) 110–121, doi:10.1016/j.virusres.2012.11.009.

[33] L Ferrari, P Borghetti, E De Angelis, P Martelli, Memory T cell proliferative responses and IFN-γ productivity sustain long-lasting efficacy of a Cap-based PCV2 vaccine upon PCV2 natural infection and associated disease, Vet. Res. 45 (2014) 44, doi:10.1186/1297-9716-45-44.

[34] S C Talker, T Käser, K Reutner, C Sedlak, K H Mair, H Koinig, R Graage, M Viehmann, E Klingler, A Ladinig, M Ritzmann, A Saalmüller, W Gerner, Phenotypic maturation of porcine NK- and T-cell subsets, Dev. Comp. Immunol. 40 (2013) 51–68, doi:10.1016/j.dci.2013.01.003.

[35] T G de Bruin, E M van Rooij, Y E de Visser, J J Voermans, J N Samsom, T G Kimman, A T Bianchi, Discrimination of different subsets of cytolytic cells in pseudorabies virus-immune and naïve pigs, J. Gen. Virol. 81 (2000) 1529–1537, doi:10.1099/0022-1317-81-6-1529.

[36] C J Chung, S H Cha, A L Grimm, D Ajithdoss, J Rzepka, G Chung, J Yu, W C Davis, C S Ho, Pigs that recover from porcine reproduction and respiratory syndrome virus infection develop cytotoxic CD4$^+$CD8$^+$ and CD4$^+$CD8$^-$ T-cells that kill virus infected cells, PLoS One 13 (2018) e0203482, doi:10.1371/journal.pone.0203482.

[37] L Ferrari, P Borghetti, G Ferrarini, E De Angelis, E Canelli, G Ogno, A Catella, T Ciociola, W Magliani, P Martelli, Phenotypic modulation of porcine CD14 + monocytes, natural killer/natural killer T cells and CD8αβ + T cell subsets by an antibody-derived killer peptide (KP), Res. Vet. Sci. 109 (2016) 29–39, doi:10.1016/j.rvsc.2016.09.008.

[38] L Ferrari, P Martelli, R Saleri, E De Angelis, V Cavalli, M Bresaola, M Benetti, P Borghetti, Lymphocyte activation as cytokine gene expression and secretion is related to the porcine reproductive and respiratory syndrome virus (PRRSV) isolate after in vitro homologous and heterologous recall of peripheral blood mononuclear cells (PBMC) from pigs vaccinated and exposed to natural infection, Vet. Immunol. Immunopathol. 151 (2013) 193–206, doi:10.1016/j.vetimm.2012.11.006.

[39] L Polonelli, W Magliani, S Conti, L Bracci, L Lozzi, P Neri, D Adriani, F De Bernardis, A Cassone, Therapeutic activity of an engineered synthetic killer antiidiotypic antibody fragment against experimental mucosal and systemic candidiasis, Infect. Immun. 71 (2003) 6205–6212, doi:10.1128/iai.71.11.6205-6212.2003.

[40] H R Juul-Madsen, K H Jensen, J Nielsen, B M Damgaard, Ontogeny and characterization of blood leukocyte subsets and serum proteins in piglets before and after weaning, Vet. Immunol. Immunopathol. 133 (2010) 95–108, doi:10.1016/j.vetimm.2009.07.006.

[41] E Canelli, A Catella, P Borghetti, L Ferrari, G Ogno, E De Angelis, P Bonilauri, S Guazzetti, R Nardini, P Martelli, Efficacy of a modified-live virus vaccine in pigs experimentally infected with a highly pathogenic porcine reproductive and respiratory syndrome virus type 1 (HP-PRRSV-1), Vet. Microbiol. 226 (2018) 89–96, doi:10.1016/j.vetmic.2018.10.001.

[42] A Y Karulin, R Caspell, M Dittrich, P V Lehmann, Normal distribution of CD8 T-cell-derived ELISPOT counts within replicates justifies the reliance on parametric statistics for identifying positive responses, Cells 4 (2015) 96–111, doi:10.3390/cells4010096.

[43] S Chamorro, C Revilla, B Alvarez, F Alonso, A Ezquerra, J Domínguez, Phenotypic and functional heterogeneity of porcine blood monocytes and its relation with maturation, Immunol. 114 (2005) 63–71, doi:10.1111/j.1365-2567.2004.01994.x.

[44] P Ondrackova, J Matiasovic, J Volf, J Dominguez, M Faldyna, Phenotypic characterisation of the monocyte subpopulations in healthy adult pigs and Salmonella-infected piglets by seven-colour flow cytometry, Res. Vet. Sci. 94 (2013) 240–245, doi:10.1016/j.rvsc.2012.09.006.

[45] F Soldevila, J C Edwards, S P Graham, L M Stevens, B Crudgington, H R Crooke, D Werling, F Steinbach, Characterization of the myeloid cell populations resident in the porcine palatine tonsil, Front. Immunol. 9 (2018) 1800, doi:10.3389/fimmu.2018.01800.

[46] E Gabrielli, E Pericolini, E Cenci, F Ortelli, W Magliani, T Ciociola, F Bistoni, S Conti, A Vecchiarelli, L Polonelli, Antibody complementarity-determining regions (CDRs): a bridge between adaptive and innate immunity, PLoS One 4 (2009) e8187, doi:10.1371/journal.pone.0008187.

[47] E Gabrielli, E Pericolini, E Cenci, C Monari, W Magliani, T Ciociola, S Conti, R Gatti, F Bistoni, L Polonelli, A Vecchiarelli, Antibody constant region peptides can display immunomodulatory activity through activation of the Dectin-1 signalling pathway, PLoS One 7 (2012) e43972, doi:10.1371/journal.pone.0043972.

[48] G J Renukaradhya, C Manickam, M Khatri, A Rauf, X Li, M Tsuji, G Rajashekara, V Dwivedi, Functional invariant NKT cells in pig lungs regulate the airway hyperreactivity: a potential animal model, J. Clin. Immunol. 31 (2011) 228–239, doi:10.1007/s10875-010-9476-4.

[49] S Werwitzke, A Tiede, B E Drescher, R E Schmidt, T Witte, CD8β/CD28 expression defines functionally distinct populations of peripheral blood T lymphocytes, Clin. Exp. Immunol. 133 (2003) 332–343, doi:10.1046/j.1365-2249.2003.02226.x.

[50] D Thakral, J Dobbins, L Devine, P B Kavathas, Differential expression of the human CD8beta splice variants and regulation of the M-2 isoform by ubiquitination, J. Immunol. 180 (2008) 7431–7442, doi:10.4049/jimmunol.180.11.7431.

[51] D Thakral, M M Coman, A Bandyopadhyay, S Martin, J L Riley, P B Kavathas, The human CD8β M-4 isoform dominant in effector memory T cells has distinct cytoplasmic motifs that confer unique properties, PLoS One 8 (2013) e59374, doi:10.1371/journal.pone.0059374.

[52] S G Kitchen, J K Whitmire, N R Jones, Z Galic, C M Kitchen, R Ahmed, J A Zack, The CD4 molecule on CD8 + T lymphocytes directly enhances the immune response to viral and cellular antigens, Proc. Natl. Acad. Sci. U.S.A. 102 (2005) 3794–3799, doi:10.1073/pnas.0406603102.

[53] M Pintarič, W Gerner, A Saalmüller, Synergistic effects of IL-2, IL-12 and IL-18 on cytolytic activity, perforin expression and IFN-gamma production of porcine natural killer cells, Vet. Immunol. Immunopathol. 121 (2008) 68–82, doi:10.1016/j.vetimm.2007.08.009.

[54] W Jennes, L Kestens, D F Nixon, B L Shacklett, Enhanced ELISPOT detection of antigen-specific T cell responses from cryopreserved specimens with addition of both IL-7 and IL-15 – the Amplispot assay, J. Immunol. Methods 270 (2002) 99–108, doi:10.1016/s0022-1759(02)00275-2.

[55] P A Ott, B R Berner, B A Herzog, R Guerkov, N L Yonkers, I Durinovic-Bello, M Tary-Lehmann, P V Lehmann, D D Anthony, CD28 costimulation enhances the sensitivity of the ELISPOT assay for detection of antigen-specific memory effector CD4 and CD8 cell populations in human diseases, J. Immunol. Methods 285 (2004) 223–235, doi:10.1016/j.jim.2003.12.007.

[56] S Kuerten, T R Schlingmann, T Rajasalu, D N Angelov, P V Lehmann, M Tary-Lehmann, Lack of disease specificity limits the usefulness of in vitro costimulation in HIV- and HCV-infected patients, Clin. Dev. Immunol. 2008 (2008) 590941, doi:10.1155/2008/590941.

[57] G Huang, X Liu, D W Duszynski, X Tang, S El-Ashram, Z Liu, X Suo, Q Li, Improved cytotoxic T lymphocyte responses to vaccination with porcine reproductive and respiratory syndrome virus in 4-1BB transgenic pigs, Front. Immunol. 8 (2017) 1846, doi:10.3389/fimmu.2017.01846.

[58] Q M Cao, Y Y Ni, D Cao, D Tian, D M Yugo, C L Heffron, C Overend, S Subramaniam, A J Rogers, N Catanzaro, T LeRoith, P C Roberts, X J Meng, Recombinant porcine reproductive and respiratory syndrome virus expressing membrane-bound interleukin-15 as an immunomodulatory adjuvant enhances NK and γδ T cell responses and confers heterologous protection, J. Virol. 92 (2018), doi:10.1128/JVI.00007-18.

[59] S L Waldrop, K A Davis, V C Maino, L J Picker, Normal human CD4 + memory T cells display broad heterogeneity in their activation threshold for cytokine synthesis, J. Immunol. 161 (1998) 5284–5295.

[60] M D Hesse, A Y Karulin, B O Boehm, P V Lehmann, M Tary-Lehmann, A T cell clone's avidity is a function of its activation state, J. Immunol. 167 (2001) 1353–1361, doi:10.4049/jimmunol.167.3.1353.

[61] R Chandwani, K A Jordan, B L Shacklett, E Papasavvas, L J Montaner, M G Rosenberg, D F Nixon, J K Sandberg, Limited magnitude and breadth in the HLA-A2-restricted CD8 T-cell response to Nef in children with vertically acquired HIV-1 infection, Scand. J. Immunol. 59 (2004) 109–114, doi:10.1111/j.0300-9475.2004.01365.x.

[62] S C Talker, H C Koinig, M Stadler, R Graage, E Klingler, A Ladinig, K H Mair, S E Hammer, H Weissenböck, R Dürrwald, M Ritzmann, A Saalmüller, W Gerner, Magnitude and kinetics of multifunctional CD4 + and CD8β + T cells in pigs infected with swine influenza A virus, Vet. Res. 46 (2015) 52, doi:10.1186/s13567-015-0182-3.

[63] S C Talker, M Stadler, H C Koinig, K H Mair, I M Rodríguez-Gómez, R Graage, R Zell, R Dürrwald, E Starick, T Harder, H Weissenböck, B Lamp, S E Hammer, A Ladinig, A Saalmüller, W Gerner, Influenza A virus infection in pigs attracts multifunctional and cross-reactive T cells to the lung, J. Virol. 90 (2016) 9364–9382, doi:10.1128/JVI.01211-16.

[64] W Zhang, P V Lehmann, Objective, user-independent ELISPOT data analysis based on scientifically validated principles, Methods Mol. Biol. 792 (2012) 155–171, doi:10.1007/978-1-61779-325-7_13.

[65] S Janetzki, L Price, H Schroeder, C M Britten, M J Welters, A Hoos, Guidelines for the automated evaluation of Elispot assays, Nat. Protoc. 10 (2015) 1098–1115, doi:10.1038/nprot.2015.068.